LANGMUIR

pubs.acs.org/Langmuir Article

Photoelectrochemical Aptasensors Constructed with Photosensitive PbS Quantum Dots/TiO_2 Nanoparticles for Detection of Kanamycin

Yichen Xing, Xiaoxiao Chen, Boxing Jin, Piaopiao Chen, Chaobiao Huang,* and Zhigang Jin*

Cite This: *Langmuir* 2021, 37, 3612–3619 Read Online

ACCESS | Metrics & More | Article Recommendations

ABSTRACT: Kanamycin (Kana) is widely used as a veterinary medicine and its abuse causes a serious threat to human health, raising the urgent demand for detection of residual Kana in animal-derived food with high specificity and sensitivity. Here, we developed a photoelectrochemical (PEC) biosensor for rapid quantification of Kana, with lead sulfide quantum dots/titanium dioxide nanoparticles (PbS QDs/TiO_2 NPs) as a photosensitive composite, a Kana-specific DNA aptamer as a functional sensor, and ruthenium(III) hexaammine ($Ru(NH_3)_6^{3+}$) as a signal booster. To prepare the PEC aptasensor, TiO_2 NPs, PbS QDs, and polyethyleneimine (PEI) were respectively used to modify the indium tin oxide electrode, and then the amine-terminated aptamer probe was connected to the PEI via glutaraldehyde. Finally, $Ru(NH_3)_6^{3+}$ was attached on the surface of the aptamer to increase the photocurrent intensity. When Kana binds competitively with $Ru(NH_3)_6^{3+}$ to the aptamer immobilized on the surface of the aptasensor, $Ru(NH_3)_6^{3+}$ will be released from the aptamer, resulting in a decrease of the photocurrent signal. This PEC aptasensor exhibits a good linear relationship between the photocurrent shift and the logarithm of Kana concentration within the range of 1.0−300.0 nmol L^{-1}, and the detection limit is 0.161 nmol L^{-1}. Importantly, the PEC aptasensor presented good detection selectivity owing to specific interaction with Kana and was successfully implemented to quantify Kana in honey and milk, suggesting that the PEC aptasensor has the potential of rapid detection of residual Kana in animal-derived foods.

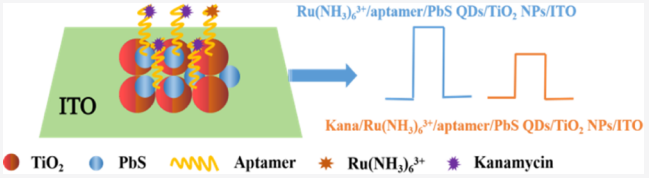

INTRODUCTION

Kanamycin (Kana), an aminoglycoside antibiotic, is broadly used as a veterinary medicine to prevent or treat infectious diseases. However, persistent abuse of Kana may result in residues in animal-derived foods (such as honey and milk),[1] which could be ultimately accumulated in the human body via the food chain, causing adverse side effects (such as neurotoxicity and nephrotoxicity) and antimicrobial resistance.[2] Therefore, the limitation of Kana residues in animal-derived products has been gradually standardized and globalized for food safety and human health. The EU and China have set the maximum residue limit of Kana in food at 150 and 200 μg/kg.[3]

Up to the present, a series of analytical techniques have been proposed to detect Kana, for example, high-performance liquid chromatography,[4] capillary electrophoresis,[5] spectrophotometry,[6,7] enzyme-linked immunosorbent assay.[8] Although these methods can effectively detect residual Kana, they are limited by cumbersome operations, time-consuming, expensive equipment, low sensitivity or specificity. Therefore, there is a pressing demand to expand a cost-effective, sensitive and fast method for detecting Kana in animal-derived food to ensure public health.

In recent years, photoelectrochemical (PEC) biosensors have been developed rapidly due to the excellent analytical characteristics including high detection sensitivity and low background noise.[9−11] At present, PEC biological analysis mainly includes DNA analysis,[12] immunoassay,[13] enzymatic sensing,[14] and cell-related detection.[15] Among them, DNA analysis has been the most extensively studied. The detection performance of the PEC biosensor is closely related to its surface-modified photosensitive material. Common photosensitive materials include inorganic semiconductor materials and organic semiconductor materials such as TiO_2, CdS quantum dots (QDs), and g-C_3N_4.[16−18]

TiO_2 has good biocompatibility, high chemical stability, low toxicity, and is widely used in the development of PEC biosensors.[19] However, TiO_2 has a large band gap (E_g = 3.2 eV) and can be effectively excited by ultraviolet light, which limits its conversion efficiency and sensitivity of PEC biosensors.[20] To address this issue, one of the most feasible ways is to combine TiO_2 with semiconductors with a high conduction band energy level and a narrow band gap. Lead sulfide QDs (PbS QDs) are a good selection because of their

Received: December 20, 2020
Revised: March 9, 2021
Published: March 17, 2021

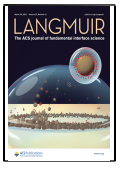

https://doi.org/10.1021/acs.langmuir.0c03593
Langmuir 2021, 37, 3612−3619

Scheme 1. Mechanism Diagram of a PEC Aptasensor Based on PbS QDs/TiO_2 NPs for the Detection of Kana; (a) In Electrolyte without Kana, the PEC Aptasensor Produces a Photocurrent Signal; (b) In Electrolyte with Kana, the Photocurrent Signal Decreases as Compared to (a), Leading to a Kana Concentration-Dependent Photocurrent Shift

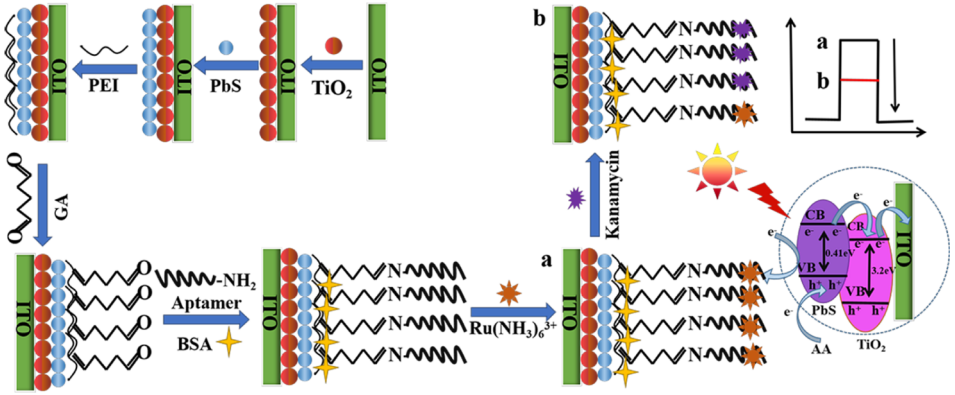

large exciton Bohr radius (18 nm) and their narrow band gap ($E_g \approx 0.41$ eV), which leads to extensive quantum size effects. Owing to multiple exciton generation and efficient spatial separation of the photo-generated charge that hinders the recombination of electron−hole (e^-−h^+), PbS QDs can further enhance the photoelectric activity of TiO_2.[21] Therefore, combining the large band gap of TiO_2 with the small band gap of PbS QDs can improve the photoelectric conversion efficiency and sensitivity of PEC biosensors.[22]

Aptamers are artificial single-stranded oligonucleotides that can be synthesized easily and inexpensively by chemical methods. In a typical configuration of aptamer-based aptasensors, the aptamer is fixed on the sensor surface for specific recognition and binding to the target substance, which could be recorded by the sensor as signal changes.[23,24] Due to the excellent sensitivity, selectivity, and stability, aptasensors have been widely employed to detect contaminants and pollutants in different fields such as antibiotics,[25,26] metal ions,[27] and hormones.[28−30]

In this study, we proposed a PEC biosensor for rapid quantification of Kana. A high-temperature calcination method is used to modify titanium dioxide nanoparticles (TiO_2 NPs) on the surface of the indium tin oxide (ITO) electrode, and PbS QDs are modified on the electrode surface through successive ionic layer adsorption and reaction (SILAR) cycles to obtain the PbS QDs/TiO_2 NPs/ITO electrode. A novel PEC aptasensor was produced via immobilization of the amine-terminated Kana aptamer to the surface of polyethyleneimine (PEI)/PbS QDs/TiO_2 NPs/ITO. As shown in Scheme 1, the principle of the developed PEC aptasensor is based on the competitive binding of Kana and $Ru(NH_3)_6^{3+}$ to the immobilized Kana-specific aptamer being converted to a change of the photocurrent signal. Finally, the PEC aptasensor exhibited desirable performance during quantification of Kana in honey and milk.

EXPERIMENTAL SECTION

Material and Reagents. Sodium sulfide (Na_2S), lead nitrate ($Pb(NO_3)_2$), methanol (CH_4O), potassium chloride (KCl), sodium hydroxide (NaOH), sodium chloride (NaCl), glutaraldehyde (GA 25% aqueous solution), and *n*-hexane (C_6H_{14}) were acquired from Sinopharm Chemical Reagent Co. Ltd., China; hexaammine ruthenium(III) chloride ($Ru(NH_3)_6Cl_3$) was obtained from Alfa Aesar Chemical Co. Ltd., China; acetonitrile (C_2H_3N) was supplied by Guangdong Guanghua Sci-Tech Co., Ltd., China; isopropanol PEI, ascorbic acid (AA), chloramphenicol (Cap), neomycin (Nom), gentamycin (Genta), and tetracycline (TC) were purchased from Aladdin Reagent Co. Ltd., China; titanium dioxide (TiO_2), Tris hydrochloride (Tris-HCl), and bovine serum albumin (BSA) were supplied by Adamas Reagent Co. Ltd., China; an electrolyte containing phosphate buffer saline (PBS, pH 7.4, 0.1 mol L^{-1} NaH_2PO_4, Na_2HPO_4, KCl) and 0.1 mmol L^{-1} AA was prepared; ITO electrodes (resistivity 6−8 Ω) were obtained from Huanan Xiangcheng Technology, Ltd., China; Kana and Kana-specific DNA aptamers with the sequences 5′-NH_2-$(CH_2)_6$-TGG-GGG-TTG-AGG-CTA-AGC-CGA-3′[16] were acquired from Sangon Biotechnology Co. Ltd., Shanghai, China. The water used in this experiment is all ultra-pure water.

Instruments. The surface morphology of the prepared materials was characterized via a scanning electron microscope (JSM-6360, JEOL, Belgium). The X-ray diffraction (XRD) pattern was acquired on an Empyrean diffractometer with a graphite monochromated Cu Kα radiation source (PANalytical B.V., The Netherlands). The X-ray photoelectron spectrometer was obtained by X-ray photoelectron spectroscopy (XPS, ESCALAB 250Xi, USA). The PEC detection was implemented at a CHI850D electrochemical workstation (CH Instruments, Shanghai, China).

Preparation of the PbS QDs/TiO_2 NPs/ITO Photosensitive Composite. The ITO electrode was dipped in a 1.0 mol L^{-1} NaOH solution and boiled for 10 min. After taking it out, it was ultrasonically cleaned with ultra-pure water and ethanol for 10 min and dried at 120 °C for 120 min. The 4.0 mg mL^{-1} TiO_2 NPs suspension dispersed by ultrasound was added drop-wise on the ITO electrode (0.5 × 0.5 cm^2), and after natural drying, it was put in a 450 °C muffle furnace and calcined for 60 min to obtain TiO_2 NPs/ITO.

The PbS QDs/TiO_2 NPs/ITO electrode was obtained via the SILAR method.[31] First, the TiO_2 NPs/ITO electrode was placed in the methanol solution containing 0.1 mol L^{-1} $Pb(NO_3)_2$ for 1 min, taken out, and rinsed with ultra-pure water to remove excessive $Pb(NO_3)_2$ precursor. Then, the electrode was placed in the methanol solution containing 0.1 mol L^{-1} Na_2S for 1 min, taken out, and rinsed with ultra-pure water to discard the excessive Na_2S precursor. The above process was termed as one SILAR cycle. After five SILAR cycles, the prepared PbS QDs/TiO_2 NPs/ITO electrode was air-dried for immediate use or storage at 4 °C in the refrigerator.

Construction of the PEC Aptasensor. The amine-terminated Kana aptamer was immobilized on the PbS QDs/TiO_2 NPs/ITO electrode by cross-linker GA. First, 3.0 μL of PEI aqueous solution (1%) was dispensed onto the surface of the PbS QDs/TiO_2 NPs/ITO. Then, 6.0 μL of GA solution (2.5%) was coated on the PEI/PbS QDs/TiO_2 NPs/ITO for 30 min and rinsed with 0.1 mol L^{-1} PBS (pH 7.4), The prepared electrode was immersed in amine-terminated Kana aptamer (2.5 μmol L^{-1}) working solution (0.1 mol L^{-1} PBS) for 4 h at 4 °C in the refrigerator to immobilize the Kana aptamer on the surface of the PEI/PbS QDs/TiO_2 NPs/ITO electrode. Next, un-

https://doi.org/10.1021/acs.langmuir.0c03593
Langmuir 2021, 37, 3612−3619

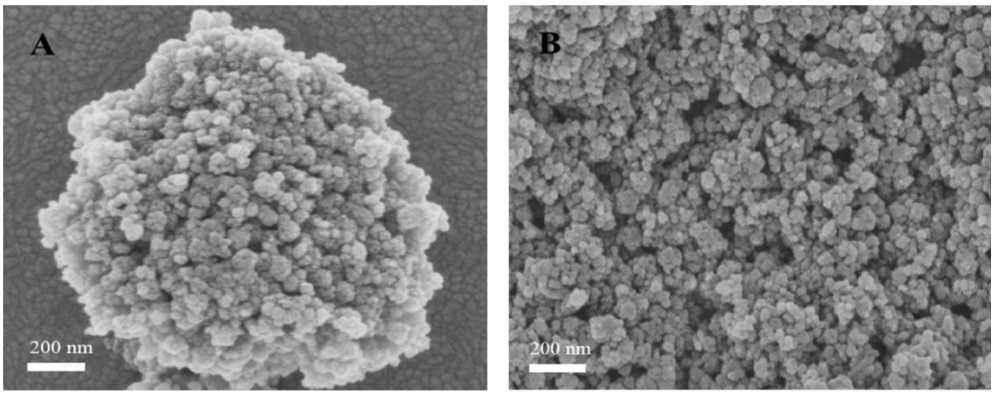

Figure 1. SEM images of (A) pure TiO_2 NPs and (B) PbS QDs/TiO_2 NP composite. Scalebar: (A,B) 200 nm.

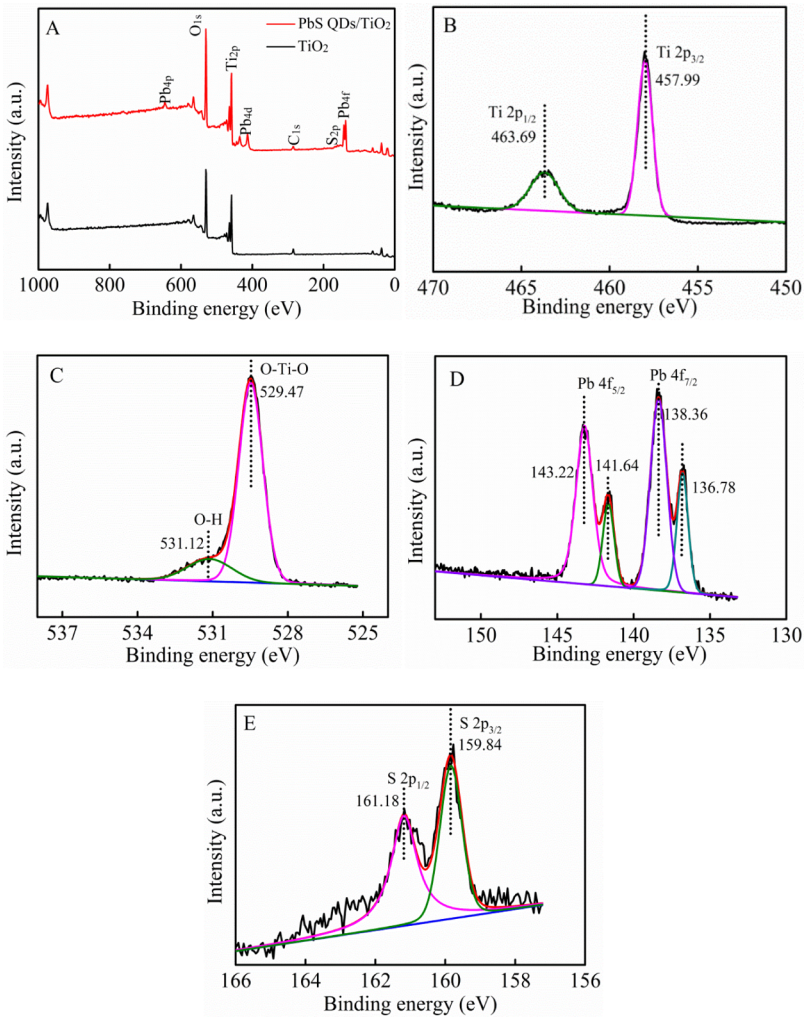

Figure 2. (A) Full-scan XPS spectra of the PbS QDs/TiO_2 NPs/ITO electrode and high-resolution XPS spectra of (B) Ti 2p; (C) O 1s; (D) Pb 4f; and (E) S 2p.

immobilized Kana aptamers were removed from the electrode by rinsing with ultra-pure water. After that, 20.0 μL of BSA solution (2%) was dropped onto the fabricated aptasensor for 1 h to block the remaining binding sites. The Kana aptamer/PEI/PbS QDs/TiO_2 NPs/ITO electrode was then rinsed thoroughly with ultra-pure water. Finally, the Kana aptamer/PEI/PbS QDs/TiO_2 NPs/ITO electrode was immersed in 0.2 mmol L^{-1} $Ru(NH_3)_6^{3+}$ for 60 min to interact with the purine of aptamer.[32]

PEC Determination. PEC detection was performed in electrolyte containing PBS and 0.1 mmol L^{-1} AA. The prepared electrode of the PEC aptasensor was immersed into the Tris-HCl buffer (20.0 mmol L^{-1} Tris-HCl, 5.0 mmol L^{-1} KCl, 50.0 mmol L^{-1} NaCl, pH 7.4) containing different concentrations of Kana and incubated for 80 min at 4 °C in a refrigerator. Next, the prepared electrode was washed with PBS solution to rinse away excessive Kana and made ready for PEC detection under 470 nm excitation wavelength.

Preparation of Real Samples. To quantify Kana in the honey sample, 2.0 g of the honey was added to a 10.0 mL container and mixed with 3.0 mL of acetonitrile solution by vortexing to precipitate excessive proteins. The supernatant was filtered by a 0.22 μm porous

https://doi.org/10.1021/acs.langmuir.0c03593
Langmuir 2021, 37, 3612−3619

membrane and made ready for detection. The whole procedure took about 30 min. To quantify Kana in the milk sample, 1.0 mL of milk was added to a 10.0 mL container and mixed with 2.5 mL of acetonitrile solution by vortexing to precipitate excessive proteins. The supernatant was transferred to a 10.0 mL container and mixed with 2.0 mL of *n*-hexane solution by vortexing. The organic phase was discarded to remove the grease and it was repeated three times. Finally, the aqueous phase was transferred into a 15.0 mL small beaker, heated, and evaporated to solid state, which was dissolved in ultra-pure water to a constant volume of 10.0 mL for PEC detection.[33] The whole procedure took about 60 min.

RESULTS AND DISCUSSION

Characterization of the PbS QDs/TiO_2 NPs. The morphology of the PbS QDs/TiO_2 NPs photosensitive composite was investigated via a scanning electron microscope. The TiO_2 NPs (Figure 1A) exhibited typical spherical NP morphology and were evenly distributed on the ITO electrode surface. In Figure 1B, the SEM of PbS QDs/TiO_2 NPs/ITO showed that the surface of TiO_2 NPs/ITO electrode was covered by PbS QDs, which is smaller in particle size. Thus, the successful preparation of the electrode was proved by SEM results.

To further verify the elemental compositions of the PbS QDs/TiO_2 NPs composite, XPS spectra were obtained. The survey scans (Figure 2A) confirmed the existence of Ti, O, Pb, and S elements in the prepared photosensitive composite. In addition, the peak positions of Ti and O elements did not shift significantly after the modification of PbS QDs. In more detail, Figure 2B shows the Ti 2p spectrum; the Ti $2p_{1/2}$ peak corresponds to 463.69 eV and the Ti $2p_{3/2}$ peak corresponds to 457.99 eV, indicating that the electrode material Ti element is in the fully oxidized state of Ti^{4+} (O−Ti−O).[34,35] The characteristic peaks at 529.47 and 531.12 eV were observed in the spectrum of O 1s (Figure 2C), which were attributed to the Ti−O bond and the hydroxyl groups on the surface or the O in the surface adsorbed water molecules.[36] As shown in Figure 2D, the binding energies of 141.64 and 138.36 eV in the high-resolution spectrum of Pb 4f corresponded to the Pb $4f_{5/2}$ and Pb $4f_{7/2}$ peaks of Pb^{2+} in PbS QDs and to the Pb−S and Pb−O bonds, respectively.[37] In Figure 2E, both peaks at 161.18 and 159.84 eV were attributed to the Pb−S bond[38,39] but specifically corresponded to S $2p_{1/2}$ and S $2p_{3/2}$, respectively. In general, the chemical state and elemental composition evaluated from the above spectra also validated that the PbS QDs/TiO_2 NPs photosensitive composite was synthesized as expected.

The crystalline structure of the photosensitive composite was analyzed by powder XRD. As shown in Figure 3a,b, for the pure TiO_2 NPs (curve a), all diffraction peaks could be attributed to the anatase TiO_2 NP phase, corresponding to the (101), (004), (105), and (211) crystallographic planes of anatase TiO_2 NPs, respectively (JCPDS no. 21-1272).[40] For the photosensitive composite (curve b), the signal peaks of the PbS (200), (220), (311), and (222) crystal planes were observed, which further proved that PbS QDs have been successfully modified to the surface of the TiO_2 NPs/ITO electrode (JPCDS no. 65-0692).[41]

PEC Behavior of the PEC Aptasensor. The rationale of Kana quantification by our PEC aptasensor is as follows: binding of $Ru(NH_3)_6^{3+}$ to an aptamer immobilized on the surface of the aptasensor will produce a photocurrent signal; when Kana binds competitively with $Ru(NH_3)_6^{3+}$ to the aptamer, $Ru(NH_3)_6^{3+}$ will be released from the aptamer,

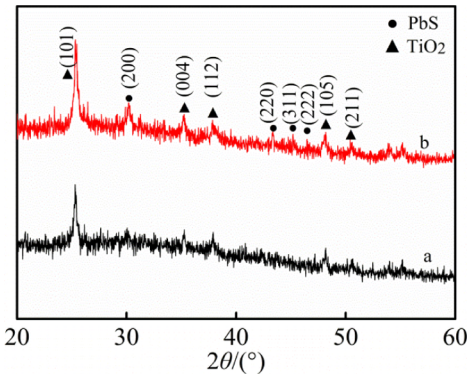

Figure 3. XRD patterns of (a) pure TiO_2 NPs and (b) PbS QDs/TiO_2 NPs composite.

resulting in a decrease of photocurrent signal in a dose-dependent manner. To confirm this, we tested different assembled electrodes for their photocurrent intensity in an electrolyte (Figure 4a−f). Among them, the bare ITO

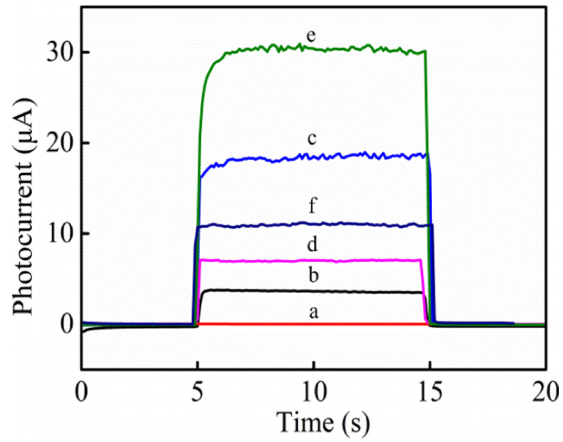

Figure 4. Photocurrent intensity: (a) pure ITO; (b) TiO_2 NPs/ITO; (c) PbS QDs/TiO_2 NPs/ITO; (d) Kana aptamer/PbS QDs/TiO_2 NPs/ITO; (e) $Ru(NH_3)_6^{3+}$/Kana aptamer/PbS QDs/TiO_2 NPs/ITO; (f) specific binding between 200.0 nmol L^{-1} Kana and the aptamer. The PEC tests were performed in an electrolyte with a 470 nm excitation light and a 0.0 V applied voltage.

electrode was unable to produce any photocurrent signal (curve a). The photocurrent was slightly enhanced using the electrode modified with TiO_2 NPs (curve b) and was further enhanced using the PbS QDs/TiO_2 NPs/ITO electrode (curve c). This could be explained by the conduction band level of PbS QDs being higher than that of TiO_2 NPs after PbS QDs are excited, e^- are transferred to TiO_2 NPs, which effectively reduces the probability of e^-−h^+ recombination. After addition of the Kana-specific DNA aptamer, the photocurrent decreased obviously (curve d), which was due to the steric hindrance effect of aptamer macromolecules on the ITO electrode surface. With the final modification, $Ru(NH_3)_6^{3+}$ adsorbed to aptamer, the photoelectron transfer pathway increased, and the e^-−h^+ separation was accelerated, which greatly increased the photocurrent intensity (curve e and Scheme 1a). After the aptasensor reacted with Kana, the photocurrent intensity decreased significantly as compared to without Kana, leading to a photocurrent shift, which was attributed to the

https://doi.org/10.1021/acs.langmuir.0c03593
Langmuir 2021, 37, 3612−3619

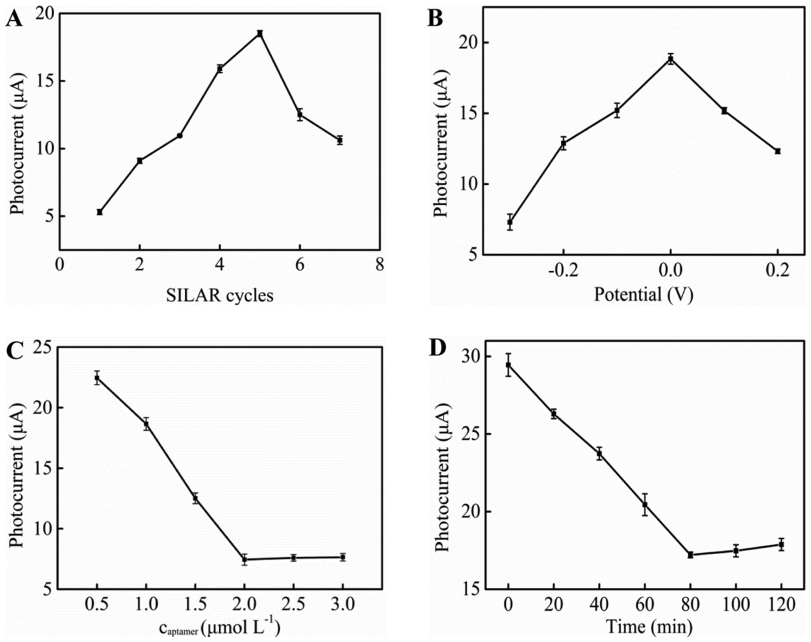

Figure 5. Optimization of the PEC aptasensor by (A) SILAR cycle times; (B) electric potential; (C) concentration of the Kana aptamer and (D) reaction time with Kana (30.0 nmol L^{-1}). Data are means ± SD (n = 3).

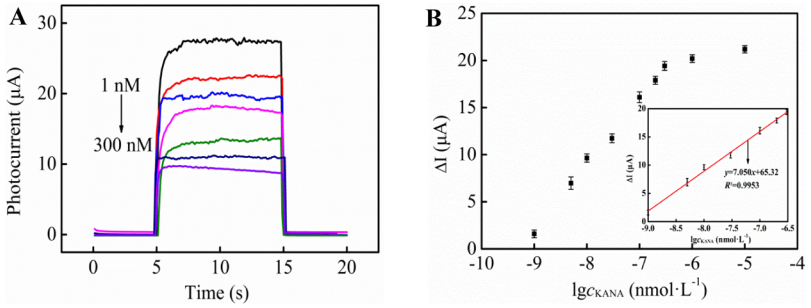

Figure 6. (A) Photocurrent shift at different contents of Kana: 1.0, 5.0, 10.0, 30.0, 100.0, 200.0, and 300.0 nmol L^{-1}; (B) linear calibration curve of photocurrent shift (Y-axis) to log c_{Kana} (X-axis).

detachment of $Ru(NH_3)_6^{3+}$ from the aptamer by Kana-mediated competition (curve f and Scheme 1b).

Optimization of PEC Aptasensor and Detection Conditions. During preparation of the PbS QDs/TiO_2 NPs/ITO electrode, PbS QDs were modified on the TiO_2 NPs/ITO electrode through SILAR cycles. However, in order to get the optimal performance PEC aptasensor, the number of SILAR cycles was optimized. Figure 5A shows the change curve of the photocurrent signal with the number of SILAR cycles. We found that the photocurrent signal increases with increasing number of SILAR cycles; but when the number is greater than 5, the photocurrent signal begins to decrease. This may be due to the excessive amount of PbS QDs modified on the ITO electrode, resulting in the increase of the electron transport path and e^-—h^+ recombination potential, and ultimately the decrease of the photocurrent signal.

The detection conditions including the electric potential, the concentration of the Kana aptamer, and the reaction time of Kana were also optimized. Figure 5B shows that as the electric potential increases, the photocurrent of the PbS QDs/TiO_2 NPs/ITO electrode increases, but when the potential exceeds 0.0 V, the photocurrent decreases with the increase of potential. This may be caused by the electrochemical oxidation of AA that occurs when the potential is over 0.0 V, leading to a weakened ability of AA to capture holes and increased possibility of electron—hole recombination.[42] Therefore, 0.0 V is selected as the detection potential. As shown in Figure 5C, with increasing concentrations of the Kana aptamer, the signal of the photocurrent gradually decreases and reaches the lowest value at 2.0 μmol L^{-1}. When the aptamer concentration increases from 2.0 to 3.0 μmol L^{-1}, the photocurrent intensity remains almost unchanged, which is mainly due to the saturation of the aptamer attached to the ITO electrode. Nevertheless, 2.0 μmol L^{-1} is the inflection point of the curve, so 2.5 μmol L^{-1} was determined as the optimal concentration of the Kana aptamer. As shown in Figure 5D, before 80 min, the photocurrent of the PEC sensor decreased rapidly with the extension of the Kana reaction time and slightly increased when the time exceeded 80 min. The reason may be that $Ru(NH_3)_6^{3+}$ is attached to the surface of the aptamer again after 80 min. Therefore, 80 min was determined as the reaction time of Kana or Kana-containing samples.

Analytical Performance of the PEC Aptasensor. Next, we investigated the relationship between PEC shift and Kana concentration under already optimized conditions. Figure 6A shows that the photocurrent intensity of the PEC aptasensor decreases as the Kana concentration increases. Figure 6B shows a good linear relationship between photocurrent shift

https://doi.org/10.1021/acs.langmuir.0c03593
Langmuir 2021, 37, 3612−3619

(change in the value of the PEC photocurrent) and log c_{Kana} when the Kana concentration ranges from 1.0 to 300.0 nmol L^{-1}, the linear equation is ΔI (μA) = 7.05 log c_{Kana} + 65.3 (R^2 = 0.9953) ($\Delta I = I_0 - I$, where I_0 and I are the photocurrent intensity without and with Kana, respectively), and the limit of detection (LOD) is 0.161 nmol L^{-1}. The performance of the constructed PEC biosensor was contrasted with many other analytical methods for Kana quantification that have been reported previously (Table 1). Compared to these analysis

Table 1. Comparison of Other Kana Quantification Methods

analytical methods	linear range (nmol L^{-1})	LOD (nmol L^{-1})	reference
high-performance liquid chromatography	10.0−150.0	25.0	43
electrochemical immunosensor	34.0−24,000.0	10.8	44
fluorescence	1.0−80.0	0.29	45
colorimetric sensing method	3.35−53.75	3.35	46
electrochemistry	10.0−500.0	1.87	47
PEC aptasensor	1.0−300.0	0.161	this study

methods, the PEC aptasensor possessed a wider linear range and lower LOD, indicating its potential application in Kana detection, especially in the scenarios where a broad detection range and high sensitivity are expected.

Specificity, Stability, and Reproducibility of the PEC Aptasensor. To explore the specificity of the aptasensor, a few representative antibiotics were selected for the interference test. During this process, the photocurrent shifts (ΔI) against individual or mixed antibiotics, including 30.0 nmol L^{-1} Kana, 300.0 nmol L^{-1} Nom, Genta, TC, and Cap, were recorded. We recruited Nom and Genta, other aminoglycoside antibiotics, into this test to check the possible cross reaction. As shown in Figure 7, a strong photocurrent shift was observed against Kana but not other individual antibiotics including Neo and Genta. Mixing all above antibiotics resulted in a photocurrent shift similar to Kana only, indicating the decent anti-interference ability of the PEC sensor under the coexistence of interfering substances. Thus, these results showed that the established PEC aptasensor has high specificity.

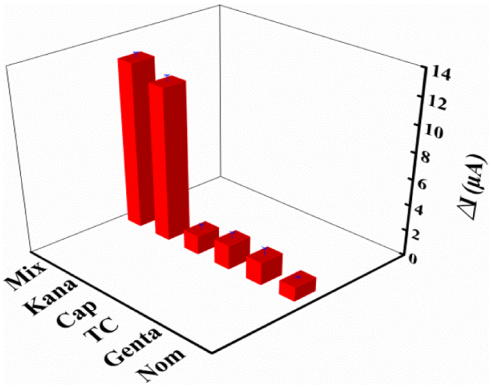

Figure 7. Specificity of the PEC aptasensor. ΔI refers to photocurrent shift ($I_0 - I$), I_0 and I are the photocurrent intensity of PEC aptasensor without and with other interfering antibiotics (300.0 nmol L^{-1})/Kana (30.0 nmol L^{-1}), respectively. Data are means ± SD (n = 3).

We also tested the PEC aptasensor for stability. As shown in Figure 8A, the photocurrent signal curve of the PEC

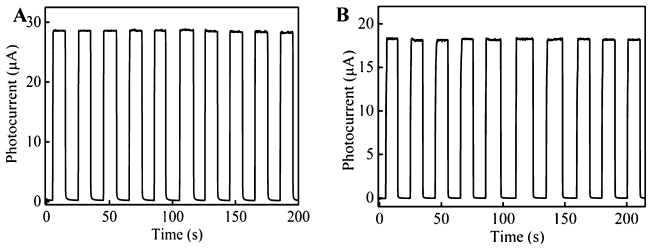

Figure 8. Stability of the PEC aptasensor (A) in the absence of Kana and (B) in the presence of Kana (30.0 nmol L^{-1}).

aptasensor was obtained under repeated 10 on/off illumination cycles for the approximately continuous 200 s in the presence of 0.0 and 30.0 nmol L^{-1} Kana. It was observed that the photocurrent signal changed very little with the extension of time, indicating that the initial value of the photocurrent signal was very stable. Figure 8B shows that the photocurrent of the aptasensor was also very stable in the presence of Kana. In addition, the reproducibility of the aptasensor was examined by a relative standard deviation (RSD) through recording the photocurrent intensity of five independent electrodes to 30.0 nmol L^{-1} Kana under the same experimental conditions. The results showed that the RSD is 3.17%, revealing that the PEC aptasensor has good reproducibility. In addition, the measured photocurrent signal of the PbS QDs/TiO_2 NPs/ITO electrode only dropped by 1.74% after storage at 4 °C for 3 weeks, indicating that the photosensitive material has good stability.

Practical Application in Animal-Derived Food. The broad detection range, high sensitivity, and specificity of the PEC aptasensor encouraged us to employ it to practically detect Kana in animal-derived food, which is one of the major fields of Kana detection. Thus, different doses of Kana (0.0, 3.0, 5.0, and 30.0 nmol L^{-1}) were added into honey and milk followed by sample preparation for PEC detection. The photocurrent shift was recorded and calculated to Kana concentration (repeated three times). Results (Table 2) showed that Kana concentration quantified by the PEC aptasensor was approximately the same as that actually added, the recovery rate was calculated as 95.4−102.2%, suggesting that the PEC aptasensor has the promising potential for Kana detection in animal-derived food.

CONCLUSIONS

In summary, we proposed a novel aptasensor for ultrasensitive determination of Kana based on a $Ru(NH_3)_6^{3+}$/Kana aptamer/PbS QDs/TiO_2 NPs/ITO electrode. PbS QDs/TiO_2 NPs/ITO electrodes were successfully prepared through a SILAR method. PbS QDs/TiO_2 NPs as a photosensitive composite can sufficiently utilize the light energy and efficaciously promote charge separation, accordingly enhancing the photocurrent conversion efficiency. The amine-terminated Kana aptamer was effectively anchored on the PEI/PbS QDs/TiO_2 NPs/ITO electrode surface via GA. $Ru(NH_3)_6^{3+}$ was attached to the electrode of the aptamer probe to increase the photocurrent intensity of the PEC aptasensor. When Kana binds competitively with $Ru(NH_3)_6^{3+}$ to the aptamer, $Ru(NH_3)_6^{3+}$ will be released from the aptamer, resulting in a decrease of the photocurrent signal. Under optimized detection conditions, the PEC aptasensor exhibited a linear

https://doi.org/10.1021/acs.langmuir.0c03593
Langmuir 2021, 37, 3612−3619

Table 2. Quantification of Kana in Real Samples Using the PEC Aptasensor

sample	added (nmol L^{-1})	found (nmol L^{-1})/($\bar{x}$ ± SD, n = 3)	recovery (%)/($\bar{x}$ ± SD, n = 3)
honey	0.000	0.000	
	3.00	3.01 ± 0.11	99.3 ± 3.7
	5.00	4.77 ± 0.15	95.4 ± 2.9
	30.0	28.97 ± 0.37	96.6 ± 1.3
milk	0.000	0.000	
	3.00	2.93 ± 0.12	97.6 ± 3.9
	5.00	5.03 ± 0.13	100.7 ± 2.5
	30.0	30.7 ± 0.38	102.2 ± 1.3

relationship between photocurrent shift and the logarithm of Kana concentration. Compared to previous methods used for Kana detection, the advantages of the PEC aptasensor include broad detection range, high sensitivity, and specificity. Importantly, the constructed PEC aptasensor was successfully applied to detect Kana in animal-derived foods such as honey and milk. The novel technique could offer a potential application in quantification of trace levels of Kana residue and evaluation of food safety.

AUTHOR INFORMATION

Corresponding Authors

Chaobiao Huang − *College of Chemistry and Life Science and Xingzhi College, Zhejiang Normal University, Jinhua 321004, China*; Email: hcb@zjnu.cn

Zhigang Jin − *College of Chemistry and Life Science, Zhejiang Normal University, Jinhua 321004, China*; orcid.org/0000-0001-7557-2968; Email: zgkin@zjnu.edu.cn

Authors

Yichen Xing − *College of Chemistry and Life Science, Zhejiang Normal University, Jinhua 321004, China*

Xiaoxiao Chen − *College of Chemistry and Life Science, Zhejiang Normal University, Jinhua 321004, China*

Boxing Jin − *College of Chemistry and Life Science, Zhejiang Normal University, Jinhua 321004, China*

Piaopiao Chen − *College of Chemistry and Life Science, Zhejiang Normal University, Jinhua 321004, China*

Complete contact information is available at: https://pubs.acs.org/10.1021/acs.langmuir.0c03593

Notes

The authors declare no competing financial interest.

ACKNOWLEDGMENTS

The present research was partially supported by the National Natural Science Foundation of China (21575129 and 31970755).

REFERENCES

(1) Strachan, C. R.; Davies, J. Antibiotics and evolution: food for thought. *J. Ind. Microbiol. Biotechnol.* **2016**, *43*, 149−153.

(2) Jiang, Y.; Sun, D.-W.; Pu, H.; Wei, Q. Ultrasensitive analysis of kanamycin residue in milk by SERS-based aptasensor. *Talanta* **2019**, *197*, 151−158.

(3) Lian, L.; Lv, J.; Wang, X.; Lou, D. Magnetic solid-phase extraction of tetracyclines using ferrous oxide coated magnetic silica microspheres from water samples. *J. Chromatogr. A* **2018**, *1534*, 1−9.

(4) Chen, S. H.; Liang, Y. C.; Chou, Y. W. Analysis of kanamycin A in human plasma and in oral dosage form by derivatization with 1-naphthyl isothiocyanate and high-performance liquid chromatography. *J. Sep. Sci.* **2006**, *29*, 607−612.

(5) Chen, X.; Hong, F.; Cao, Y.; Hu, F.; Wu, Y.; Wu, D.; Li, T.; Lin, J.; Gan, N. A microchip electrophoresis-based assay for ratiometric detection of kanamycin by R-shape probe and exonuclease-assisted signal amplification. *Talanta* **2018**, *189*, 494−501.

(6) Wang, J.; Lu, T.; Hu, Y.; Wang, X.; Wu, Y. A label-free and carbon dots based fluorescent aptasensor for the detection of kanamycin in milk. *Spectrochim. Acta, Part A* **2020**, *226*, 117651.

(7) Zhou, Y.; Zuo, L.; Wei, Y.; Dong, C. Development of fluorescent aptasensing system for ultrasensitive analysis of kanamycin. *J. Lumin.* **2020**, *222*, 117124.

(8) Loomans, E. E. M. G.; Van Wiltenburg, J.; Koets, M.; Van Amerongen, A. Neamin as an immunogen for the development of a generic ELISA detecting gentamicin, kanamycin, and neomycin in milk. *J. Agric. Food Chem.* **2003**, *51*, 587−593.

(9) Zhang, L.; Shen, Y. L.; Fan, G. C.; Xiong, M.; Yu, X. D.; Zhao, W. W. Preparation of an AgI/$CuBi_2O_4$ heterojunction on a fluorine-doped tin oxide electrode for cathodic photoelectrochemical assays: application to the detection of L-cysteine. *Mikrochim. Acta* **2019**, *186*, 284.

(10) Tang, J.; Li, J.; Xiong, P.; Sun, Y.; Zeng, Z.; Tian, X.; Tang, D. Rolling circle amplification promoted magneto-controlled photoelectrochemical biosensor for organophosphorus pesticides based on dissolution of core-shell MnO_2 nanoflower@CdS mediated by butyrylcholinesterase. *Mikrochim. Acta* **2020**, *187*, 450.

(11) Zhao, Y.; Wu, R.; Yu, H.; Li, J.; Liu, L.; Wang, S.; Chen, X.; Chan, T. W. D. Magnetic solid-phase extraction of sulfonamide antibiotics in water and animal-derived food samples using core-shell magnetite and molybdenum disulfide nanocomposite adsorbent. *J. Chromatogr. A* **2020**, *1610*, 460543.

(12) Qin, X.; Wang, Q.; Geng, L.; Shu, X.; Wang, Y. A "signal-on" photoelectrochemical aptasensor based on graphene quantum dots-sensitized TiO_2 nanotube arrays for sensitive detection of chloramphenicol. *Talanta* **2019**, *197*, 28−35.

(13) Wu, Y.; Su, H.; Yang, J.; Wang, Z.; Li, D.; Sun, H.; Guo, X.; Yin, S. Photoelectrochemical immunosensor for sensitive detection of alpha-fetoprotein based on a graphene honeycomb film. *J. Colloid Interface Sci.* **2020**, *580*, 583−591.

(14) Liang, D.; Luo, J.; Huang, Y.; Liang, X.; Qiu, X.; Wang, J.; Yang, M. A porous carbon nitride modified with cobalt phosphide as an efficient visible-light harvesting nanocomposite for photoelectrochemical enzymatic sensing of glucose. *Microchim. Acta* **2019**, *186*, 856.

(15) Zhang, X.; Liu, M.; Liu, H.; Zhang, S. Low-toxic Ag_2S quantum dots for photoelectrochemical detection glucose and cancer cells. *Biosens. Bioelectron.* **2014**, *56*, 307−312.

(16) Liu, X.; Liu, P.; Tang, Y.; Yang, L.; Li, L.; Qi, Z.; Li, D.; Wong, D. K. Y. A photoelectrochemical aptasensor based on a 3D flower-like TiO_2-MoS_2-gold nanoparticle heterostructure for detection of kanamycin. *Biosens. Bioelectron.* **2018**, *112*, 193−201.

(17) Tang, Y.; Chai, Y.; Liu, X.; Li, L.; Yang, L.; Liu, P.; Zhou, Y.; Ju, H.; Cheng, Y. A photoelectrochemical aptasensor constructed with core-shell CuS-TiO_2 heterostructure for detection of microcystin-LR. *Biosens. Bioelectron.* **2018**, *117*, 224−231.

(18) Li, Z.; Dong, W.; Du, X.; Wen, G.; Fan, X. A novel photoelectrochemical sensor based on g-C_3N_4@CdS QDs for sensitive detection of Hg^{2+}. *Microchem. J.* **2020**, *152*, 104259.

(19) Bhat, S. S. M.; Jun, S. E.; Lee, S. A.; Lee, T. H.; Jang, H. W. Influence of C_3N_4 Precursors on Photoelectrochemical Behavior of TiO_2/C_3N_4 Photoanode for Solar Water Oxidation. *Energies* **2020**, *13*, 974.
(20) Tao, J.; Sun, Z.; Cheng, Y.; Zhang, M.; Lv, J.; Shi, S.; He, G.; Jiang, X.; Chen, X.; Wang, X.; Wang, Z.; Gong, Z. Enhanced photoelectrochemical properties of nanocrystalline TiO_2 electrode by surface sensitization with Cu_xO quantum dots. *Sci. Rep.* **2017**, *7*, 5291.
(21) Ratanatawanate, C.; Xiong, C.; Balkus, K. J., Jr. Fabrication of PbS quantum dot doped TiO_2 nanotubes. *ACS Nano* **2008**, *2*, 1682−1688.
(22) Xia, H.; Wu, S.; Zhang, S. Controlled Synthesis of Hollow PbS-TiO_2 Hybrid Structures through an Ion Adsorption-Heating Process and their Photocatalytic Activity. *Chem.—Asian J.* **2017**, *12*, 2942−2949.
(23) Phanchai, W.; Srikulwong, U.; Chompoosor, A.; Sakonsinsiri, C.; Puangmali, T. Insight into the Molecular Mechanisms of AuNP-Based Aptasensor for Colorimetric Detection: A Molecular Dynamics Approach. *Langmuir* **2018**, *34*, 6161−6169.
(24) Kassahun, G. S.; Griveau, S.; Juillard, S.; Champavert, J.; Ringuedé, A.; Bresson, B.; Tran, Y.; Bedioui, F.; Slim, C. Hydrogel Matrix-Grafted Impedimetric Aptasensors for the Detection of Diclofenac. *Langmuir* **2020**, *36*, 827−836.
(25) Zhou, J.; Li, Y.; Wang, W.; Lu, Z.; Han, H.; Liu, J. Kanamycin Adsorption on Gold Nanoparticles Dominates Its Label-Free Colorimetric Sensing with Its Aptamer. *Langmuir* **2020**, *36*, 11490−11498.
(26) Tian, L.; Zhang, Y.; Wang, L.; Geng, Q.; Liu, D.; Duan, L.; Wang, Y.; Cui, J. Ratiometric Dual Signal-Enhancing-Based Electrochemical Biosensor for Ultrasensitive Kanamycin Detection. *ACS Appl. Mater. Interfaces* **2020**, *12*, 52713−52720.
(27) Niu, Y.; Xie, H.; Luo, G.; Zhuang, Y.; Wu, X.; Li, G.; Sun, W. ZnO-reduced graphene oxide composite based photoelectrochemical aptasensor for sensitive Cd(II) detection with methylene blue as sensitizer. *Anal. Chim. Acta* **2020**, *1118*, 1−8.
(28) Liu, S.; Cheng, R.; Chen, Y.; Shi, H.; Zhao, G. A simple one-step pretreatment, highly sensitive and selective sensing of 17β-estradiol in environmental water samples using surface-enhanced Raman spectroscopy. *Sens. Actuators, B* **2018**, *254*, 1157−1164.
(29) Liu, S.; Chen, Y.; Wang, Y.; Zhao, G. Group-Targeting Detection of Total Steroid Estrogen Using Surface-Enhanced Raman Spectroscopy. *Anal. Chem.* **2019**, *91*, 7639−7647.
(30) Fan, L.; Zhao, G.; Shi, H.; Liu, M.; Wang, Y.; Ke, H. A Femtomolar Level and Highly Selective 17β-estradiol Photoelectrochemical Aptasensor Applied in Environmental Water Samples Analysis. *Environ. Sci. Technol.* **2014**, *48*, 5754−5761.
(31) Mustakim, N. S. M.; Ubani, C. A.; Sepeai, S.; Ludin, N. A.; Teridi, M. A. M.; Ibrahim, M. A. Quantum dots processed by SILAR for solar cell applications. *Sol. Energy* **2018**, *163*, 256−270.
(32) Lopes, L. M. F.; Garcia, A. R.; Brogueira, P.; Ilharco, L. M. Interactions between DNA Purines and Ruthenium Ammine Complexes within Nanostructured Sol−Gel Silica Matrixes. *J. Phys. Chem. B* **2010**, *114*, 3987−3998.
(33) Tu, C.; Guo, Y.; Dai, Y.; Wei, W.; Wang, W.; Wu, L.; Wang, A. Determination of Chloramphenicol in Honey and Milk by HPLC Coupled with Aptamer-Functionalized Fe_3O_4/Graphene Oxide Magnetic Solid-Phase Extraction. *J. Food Sci.* **2019**, *84*, 3624−3633.
(34) Hajjaji, A.; Jemai, S.; Rebhi, A.; Trabelsi, K.; Gaidi, M.; Alhazaa, A. N.; Al-Gawati, M. A.; El Khakani, M. A.; Bessais, B. Enhancement of photocatalytic and photoelectrochemical properties of TiO_2 nanotubes sensitized by SILAR—Deposited PbS nanoparticles. *J. Materiomics* **2020**, *6*, 62−69.
(35) Bhat, T. S.; Mali, S. S.; Sheikh, A. D.; Korade, S. D.; Pawar, K. K.; Hong, C. K.; Kim, J. H.; Patil, P. S. TiO_2/PbS/ZnS heterostructure for panchromatic quantum dot sensitized solar cells synthesized by wet chemical route. *Opt. Mater.* **2017**, *73*, 781−792.
(36) Mali, S. S.; Desai, S. K.; Kalagi, S. S.; Betty, C. A.; Bhosale, P. N.; Devan, R. S.; Ma, Y. R. R.; Patil, P. S. PbS quantum dot sensitized anatase TiO_2 nanocorals for quantum dot-sensitized solar cell applications. *Dalton Trans.* **2012**, *41*, 6130−6136.
(37) Zhang, H.; Gao, Y.; Zhu, G.; Li, B.; Gou, J.; Cheng, X. Synthesis of PbS/TiO_2 nano-tubes photoelectrode and its enhanced visible light driven photocatalytic performance and mechanism for purification of 4-chlorobenzoic acid. *Sep. Purif. Technol.* **2019**, *227*, 115697.
(38) Liu, Y.; Wang, L.; Wang, H.; Xiong, M.; Yang, T.; Zakharova, G. S. Highly sensitive and selective ammonia gas sensors based on PbS quantum dots/TiO_2 nanotube arrays at room temperature. *Sens. Actuators, B* **2016**, *236*, 529−536.
(39) Song, S.; Liang, Z.; Fu, W.; Peng, T. Preparation of Single-Crystalline $AgIn_5S_8$ Octahedrons with Exposed {111} Facets and Its Visible-Light-Responsive Photocatalytic H_2 Production Activity. *ACS Appl. Mater. Interfaces* **2017**, *9*, 17013−17023.
(40) Yang, K.; Huang, K.; He, Z.; Chen, X.; Fu, X.; Dai, W. Promoted effect of PANI as electron transfer promoter on CO oxidation over Au/TiO_2. *Appl. Catal., B* **2014**, *158−159*, 250−257.
(41) Qiao, J.; Wang, Q.; Xiao, Y. High-efficiency photoelectrochemical performance of PbS nanoparticles sensitized TiO_2 nanotube arrays. *J. Appl. Electrochem.* **2014**, *44*, 1007−1011.
(42) Yang, Y.; Jo, A.; Lee, Y.; Lee, C. Electrodeposited nanoporous ruthenium oxide for simultaneous quantification of ascorbic acid and uric acid using chronoamperometry at two different potentials. *Sens. Actuators, B* **2018**, *255*, 316−324.
(43) Blanchaert, B.; Poderós Jorge, E.; Jankovics, P.; Adams, E.; Van Schepdael, A. Assay of Kanamycin A by HPLC with Direct UV Detection. *Chromatographia* **2013**, *76*, 1505−1512.
(44) Zhang, L. P.; Xing, Y. P.; Liu, L. H.; Zhou, X. H.; Shi, H. C. Fenton reaction-triggered colorimetric detection of phenols in water samples using unmodified gold nanoparticles. *Sens. Actuators, B* **2016**, *225*, 593−599.
(45) Soganci, T.; Ayranci, R.; Harputlu, E.; Ocakoglu, K.; Acet, M.; Farle, M.; Unlu, C. G.; Ak, M. An effective non-enzymatic biosensor platform based on copper nanoparticles decorated by sputtering on CVD graphene. *Sens. Actuators, B* **2018**, *273*, 1501−1507.
(46) Ha, N. R.; Jung, I. P.; Kim, S. H.; Kim, A. R.; Yoon, M. Y. Paper chip-based colorimetric sensing assay for ultra-sensitive detection of residual kanamycin. *Process Biochem.* **2017**, *62*, 161−168.
(47) Bi, H.; Wu, Y.; Wang, Y.; Liu, G.; Ning, G.; Xu, Z. A molecularly imprinted polymer combined with dual functional Au@Fe_3O_4 nanocomposites for sensitive detection of kanamycin. *J. Electroanal. Chem.* **2020**, *870*, 114216.

https://doi.org/10.1021/acs.langmuir.0c03593
Langmuir 2021, 37, 3612−3619